

# We are IntechOpen, the world's leading publisher of Open Access books Built by scientists, for scientists

4,800

Open access books available

122,000

International authors and editors

135M

Downloads

Our authors are among the

154

Countries delivered to

TOP 1%

most cited scientists

12.2%

Contributors from top 500 universities



WEB OF SCIENCE™

Selection of our books indexed in the Book Citation Index  
in Web of Science™ Core Collection (BKCI)

Interested in publishing with us?  
Contact [book.department@intechopen.com](mailto:book.department@intechopen.com)

Numbers displayed above are based on latest data collected.  
For more information visit [www.intechopen.com](http://www.intechopen.com)



# A New Combustion Method in a Burner with Three Separate Jets

*Mohamed Ali Mergheni, Mohamed Mahdi Belhajbrahim,  
Toufik Boushaki and Jean-Charles Sautet*

## Abstract

Oxy-flames from burners with separated jets present attractive perspectives because the separation of reactants generates a better thermal efficiency and reduction of pollutant emissions. The principal idea is to confine the fuel jet by oxygen jets to favor the mixing in order to improve the flame stability. This chapter concerns the effect of equivalence ratio on characteristics of a non-premixed oxy-methane flame from a burner with separated jets. The burner of 25 kW power is composed with three aligned jets, one central methane jet surrounded by two oxygen jets. The numerical simulation is carried out using Reynolds Average Navier-Stokes (RANS) technique with  $k-\varepsilon$  as a turbulence closure model. The eddy dissipation model is applied to take into account the turbulence-reaction interactions. The study is performed with different global equivalence ratios (0.7, 0.8 and 1). The validation of the numerical tools is done by comparison with experimental data of the stoichiometric regime ( $\Phi = 1$ ). The two lean regimes of  $\Phi = 0.7$  and 0.8 are investigated only by calculations. The velocity fields with different equivalence ratio are presented. It yields to increase of longitudinal and transverse velocity, promotes the fluctuation in interaction zone between fuel and oxygen also a better mixing quality and a decrease of the size of the recirculation zone.

**Keywords:** oxy-flame, turbulent, separated-jets, equivalence ratio, flame stability

## 1. Introduction

This chapter concerns the numerical simulation and the PIV measurements on oxy-fuel burners with three separated jets. The mixing, dynamic and the temperature fields for both reacting and non-reacting flows are investigated.

Industrial systems with combustion phenomena such as burners, aeronautical engines and gas turbines are subject to increasingly important constraints, both economically (cost reduction, improved performance, etc.) than on the environmental level (reduction of pollutant emissions), requiring the development of new techniques to respond effectively to these industrial constraints. The development passes by new method of combustion in order to reduce pollutant emissions and fuel consumption, as well as by the improvement of flame stability [3, 12]. In previous studies, significant reductions of nitric oxide emissions have been successfully achieved by using low NO<sub>x</sub> technologies or oxy-combustion systems [5].

In air combustion, nitrogen leads to high fuel consumption and low combustion efficiency because nitrogen in the air acts as energy ballast. The substitution of air with pure oxygen leads to an increase in the laminar combustion rate up to 1300%, improves the thermal efficiency, increases the adiabatic flame temperature (2200 K for CH<sub>4</sub>-Air, 3090 K in oxy-combustion) reduce fuel consumption by 50% and, from an environmental point of view, reduce the formation of nitrogen oxides by up to 95% [21].

The flames from multiple jets aligned have used in many industrial installation. Several studies have been published on the dynamic properties of non-reacting multiple jets [6, 13, 14, 17, 20]. Lee et al. [7] have studied the geometry parameters of diffusion flames and giving a number of variables such as the number of jets and the distance between the jets. Lenze et al. [8] have studied the influence of three and five non-premixed flames, with town gas and natural gas burners. Their measurements concern flame width, flame length and concentrations in confined and free multiple flames.

A new generation of highly separated fuel and oxidant injection burners is of great interest to industrialists. The idea of this burner consists of separating combustible and oxidant to dilute the reactants with combustion products before the mixing of the reactants [2, 4, 9].

For this new combustion in a burner with three separated jets, the separation of jets provides a high dilution of reactants by combustion products in the combustion chamber. Consequently, this dilution decreases the flame temperature and decline in NO<sub>x</sub> production. In the literature, it has been proven that the separation of reactants are capable to change the flow structure, the flame characteristics, generates a better thermal efficiency and as well as reduction of pollutant emissions [15, 16, 18, 19].

Salentey et al. [16] was interested in the characterization the flames from multiple jets aligned through dynamic properties (speed of the jets and distance injectors) and the flame topology (stability, length, blow ...). Lesieur et al. [9] has studied numerically the characteristics of a burner with three jets, focusing on the mixing of the jets, their dynamics and the pollutant emissions. Boushaki et al. [2] was interested on two main areas for flow, passive control with changing the diameter of the burner in order to affecting the dynamics flow; and active control requiring external energy intake through actuators while retaining the geometry of the combustion chamber.

The present chapter reports the results of a numerical and experimental investigation of the dynamic field on a burner with 25 kW power composed of three jets, one central jet of natural gas and two side jets of pure oxygen [10, 11]. One control systems, passive, is added to the basic burner to ameliorate the combustion process to ensure the stabilization of flame and as well as pollutant reductions. The passive control is based on the inclined of side oxygen jets towards the central natural gas jet in burner with three separated jets.

Few works, are investigated the effect of equivalence ratios (in lean regime) on characteristics of non-premixed oxy-methane flames from burner with separated jets. However, the aim of this contribution is to investigate numerically the effect of different equivalence ratio on the combustion characteristics of a diffusion methane oxy-flame in a stabilized separated burner.

The mixture of hydrogen and natural gas is a new mixed fuel. The use of a mixed mixture of fuel and hydrogen has the advantage of modifying very effectively the properties of the fuel while preserving the distribution facility. Due to this, the high molecular diffusivity of hydrogen, the extended flammability limits, the high laminar flame speed and the low ignition energy, the addition of hydrogen in the fuel makes it possible to work in a combustion poor. Increasing flammability limits in the presence of hydrogen offset the adverse effects of poor combustion such as local extinctions, radiation energy losses, and flame stretching [22].

## 2. Burner configuration and experimental set-up

### 2.1 Basic configuration of the burner

The configuration of the burner illustrated in **Figure 1** consists in separating the fuel and oxygen per injection in order to increase the dilution of the reactants with the combustion products before the mixing of the reagents.

This burner consists of three non-ventilated jets, one central with internal diameter  $d_g$  equal 6 mm that contains the fuel and two side jets with internal diameter  $d_{ox}$  equal 6 mm contain pure oxygen. Boushaki et al. [1] have studied this three-jet burner configuration. The separation distance between the jets ( $S$ ) used is 12 mm. The gas density equal to  $0.83 \text{ kg m}^{-3}$  and the oxygen is supplied by liquid air with a purity of 99.5% with a density of  $1.354 \text{ kg m}^{-3}$  (at 1 atm and at  $15^\circ \text{C}$ ). The thermal power ( $P$ ) of the burner is equal to 25 kW, therefore the flow rate and the output speed of the natural gas are respectively  $m_{ng} = 0.556 \text{ g s}^{-1}$  and  $U_{ng} = 27.1 \text{ ms}^{-1}$ .

The first study in this document is the control technique, consists in inclining the side oxygen jets towards the natural gas jet as shown in **Figure 1**. The angle of oxygen jets ( $\Theta$ ) compared to the vertical direction varies from 0 to  $30^\circ$  (0, 10, 20, and  $30^\circ$ ), however, we will present the effect of angle of the side oxygen jets on the dynamic fluid, for many detail you can see [2].

The combustion is carried out inside a square chamber of  $60 \times 60 \text{ cm}^2$  section and a height of 1 m. The side walls are water cooled and refractory lined inside the combustion chamber. a converging 20 cm high and a final section of  $12 \times 12 \text{ cm}$  is placed at the end of the chamber to limit the entry of air from above. In order to allow optical access to all flame zones, six windows are provided in each face of the chamber.

The Particle Image Velocimetry (PIV) was used as a measurement technique to characterize the experimental dynamic field. The PIV technique requires a laser sheet that clarifies the flow area studied a CCD camera, control equipment and an acquisition PC. The laser used is the Nd-YAG Bi-pulse with frequency 10 Hz and wavelength of 532 nm. The laser chain used is composed by a first divergent cylindrical lens and then by a second convergent spherical lens. The Mie signal emitted by the particles is collected by CCD camera of type a Lavision FlowMaster (12-bit dynamic and resolution  $1280 \times 1024$  pixels).

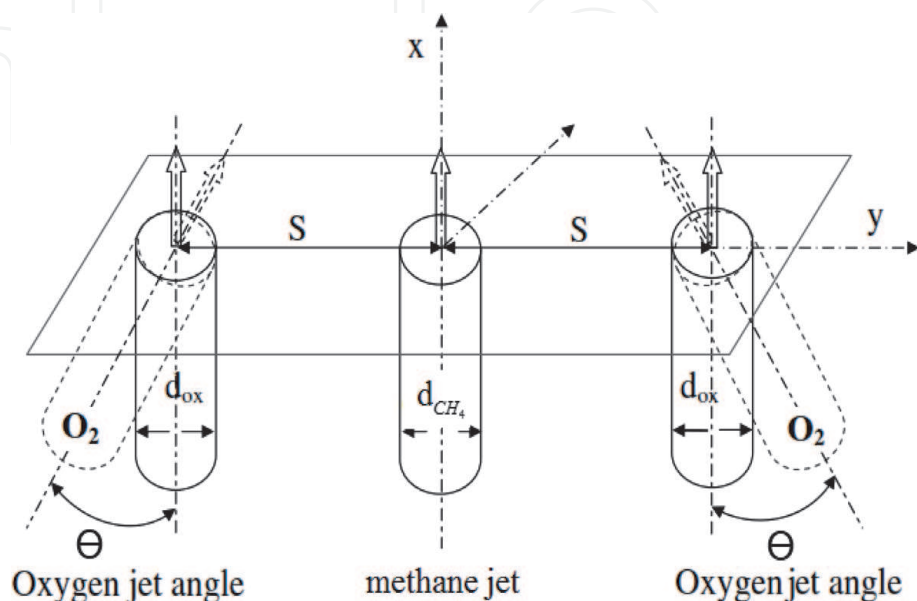


**Figure 1.**  
*Schematic view of the burner.*

### 3. Numerical method

The steady equations for conservation of mass, momentum, energy and species have been used in this numerical simulation. The second order equations for turbulence kinetic energy  $\kappa$  and its rate of dissipation  $\varepsilon$  have been used to modulate the turbulence. The general form of the elliptic differential equations for an axisymmetric flow is given by Eq. (1).

Here  $S_\Phi$  is the source term and  $\Gamma_\Phi$  is the transport coefficient.

$$\frac{\partial}{\partial x}(\rho U \Phi) + \frac{1}{r} \frac{\partial}{\partial r}(r \rho V \Phi) = \frac{\partial}{\partial x} \left( \Gamma_\Phi \frac{\partial \Phi}{\partial x} \right) + \frac{1}{r} \frac{\partial}{\partial r} \left( r \Gamma_\Phi \frac{\partial \Phi}{\partial r} \right) + S_\Phi \quad (1)$$

where  $\rho$  is the density,  $P$  is the mean pressure and  $\mu$  is the viscosity.

$\mu_e$  is the effective viscosity is determined from  $\mu_e = \mu + \mu_t$ , where  $\mu_t$  is the turbulent viscosity, which is derived from the turbulence model and expressed by:  $\mu_t = C_\mu \rho \frac{\kappa^2}{\varepsilon}$ .

The Finite Eddy Dissipation Model (EDM) is used to simulate the turbulence/chemistry interaction. This model is based on the hypothesis that the chemical reaction is fast in relation to the transport processes of the flow.

**Table 1** summarizes the volumetric flow rates, the velocities, Reynolds number respectively of methane and oxygen of equivalence ratio (0.7, 0.8 and 1).

Reynolds Number is defined by the following equation:

$$Re = (\rho d_{gn} U) / \mu \quad (2)$$

A global equivalence ratio can be defined as the molar ratio of methane and oxidant at the injection to molar ratio methane and oxidant in stoichiometric conditions, as:

$$\phi = h \left( \frac{Q}{Q_{O_2}} \right) / \left( \frac{Q_{CH_4}}{Q_{O_2}} \right)_{stoichio} \quad (3)$$

where  $Q$  is the volumetric flow rate.

The second numerical study in this document is the effect of hydrogen to dynamic of flame. One of the jet transports the fuel, natural gas + hydrogen, and the other the pure oxygen. The values of the flow rates of fuel and the exit velocities are regrouped in **Table 2**.

We shall consider an overall irreversible reaction between methane/hydrogen and pure oxygen:



$\alpha$  is the percentage of hydrogen and written as:

$$\alpha = \frac{\%H_2}{\%H_2 + \%CH_4} \quad (5)$$

Configuration	$\phi$	$\dot{Q}_{CH_4} [\frac{l}{s}]$	$\dot{Q}_{O_2} [\frac{l}{s}]$	$U_{ng} [\frac{m}{s}]$	$U_{O_2} [\frac{m}{s}]$	$Re_{gn}$
Conf1 1	1	0.767	1.534	27.13	27.13	12,272
Conf1 2	0.8	0.767	1.917	27.13	33.86	12,272
Conf1 3	0.7	0.767	2.19	27.13	38.69	12,272

**Table 1.**  
Dynamic conditions of the burner.

$\Phi = 1$					
P=25 kW					
	$\dot{m}_{CH_4}$ (g.s <sup>-1</sup> )	$\dot{m}_{H_2}$ (g.s <sup>-1</sup> )	$\dot{m}_{O_2}$ (g.s <sup>-1</sup> )	$U_{ng}$ (m.s <sup>-1</sup> )	$U_{O_2}$ (m.s <sup>-1</sup> )
0% H <sub>2</sub>	0.49	0	2.07	27.07	27.06
20% H <sub>2</sub>	0.46	0.012	2.03	31.3	26.66
40% H <sub>2</sub>	0.40	0.02	1.98	37.07	25.9

**Table 2.**  
 Flow rates and exit velocities of fuels and oxygen.

**Table 2** summarizes the parameters of this numerical study including methane, hydrogen and oxygen flow rates, velocities, percentage of hydrogen and equivalence ratio.

Fluent 6.3.2 is used to solve the steady equations for conservation of mass, momentum, energy and species. The finite volume method is used with second order upwind. In fact, convergence criterion of residuals for energy equation and for all other equations equal respectively  $10^{-6}$  and  $10^{-3}$ . The GAMBIT is used to construct the grid; the computational domain has been extended 100 cm in the axial direction and 30 cm in the radial direction. A total number of 28,700 quadrilateral cells were generated using non-uniform grid spacing to provide an adequate resolution near the jet axis and close to the burner where gradients were large.

The axial velocity profile at the inlet, of the methane is supposed constant. At the axis of symmetry,  $r = 0$ ,  $V = 0$  and  $\partial\Phi/\partial r = 0$  ( $\Phi = U, \kappa, \epsilon$ ). At the outlet, the fully-developed condition of pipe flow is adopted  $\partial\Phi/\partial x = 0$  ( $\Phi = U, V, \kappa, \epsilon$ ). The velocities are assumed to be zero at the wall, and these no-slip boundary conditions are appropriate for the gas. These equations, called “wall functions,” are introduced and used in finite difference calculations at near-wall points.

## 4. Inclined effects on dynamic

### 4.1 PIV measurements on burners with inclined jets

The mean velocity fields carried out by PIV in non-reacting flow are represented on **Figure 2**. From initial state where  $\Theta = 0^\circ$  to inclined state where  $\Theta = 30^\circ$ , the dynamic field changes with the change of flow structure. The jets fusion point

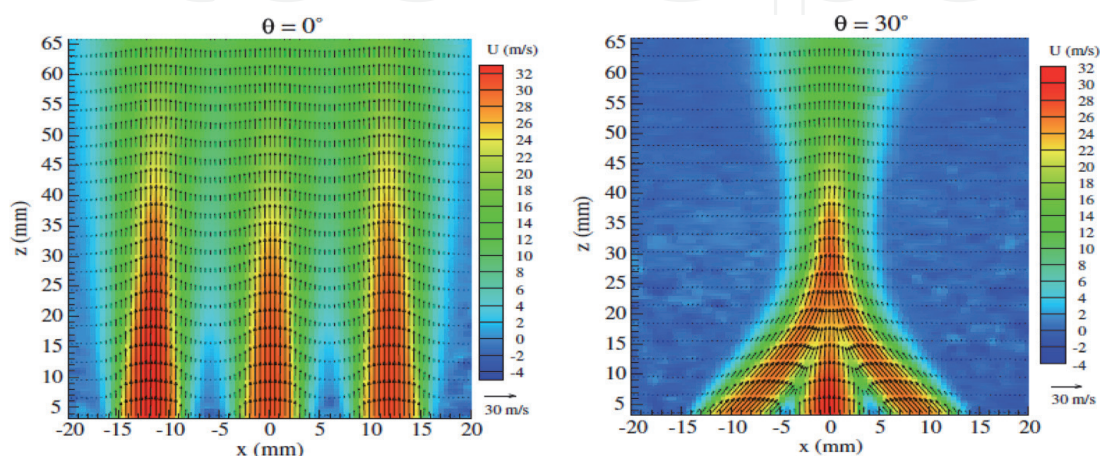


**Figure 2.**  
 Mean velocity fields for jet oxygen angle  $0^\circ$  and  $30^\circ$  (longitudinal velocity in color scale) in non-reacting flow.

becomes closer the burner by increasing of the slope of jets. The interaction of jets starts at about 15 mm for  $\Theta = 0^\circ$ , at  $z = 25$  mm for  $\Theta = 30^\circ$ .

#### 4.2 Velocity distribution and current lines

**Figure 3** shows the distribution of velocity and the current lines in the combustion chamber near the burner with different inclined jets of oxygen. In the part separating the different jets (dark blue), velocity is negative because of the recirculation of the jets. The existence of two zones of recirculation is observed with different directions of rotation, which explains the appearance of the negative velocity. It is noted on the one hand that the recirculation zone decreases with the increase of  $\Theta$  from 0 to  $20^\circ$ . This is very remarkable near the jet of oxygen. On the other hand, it can be observed that the recirculation zones appear outside the jet of air (see the lines of currents). The perturbation of velocity distribution increases with the increase of  $\Theta$ . This perturbation is accompanied by an acceleration of the combination of different jets and consequently a faster combustion reaction, which explains the increase in velocity with the increase of  $\Theta$ .

#### 4.3 Temperature distribution

The distributions of the temperature in the combustion chamber with different inclined jets are represented in **Figure 4**. It is clear here that the flame exists in the mixing zone of methane and oxygen, which represents the reaction zone. This zone is modified with the variation of the angle  $\Theta$ . If we assume that the length of the flame is defined by the red color of the flame distribution, we can conclude that the length of the flame decreases with the increase of the angle  $\Theta$  from 0.44 m for an inclination of  $0^\circ$  to 0.29 m for an inclination of  $20^\circ$  of the jet of oxygen.

**Figure 5** represents the evolution of the axial temperature at  $y = 0$  mm with different angles of injection  $\Theta$  of the oxygen jets. Firstly, it is observed that the

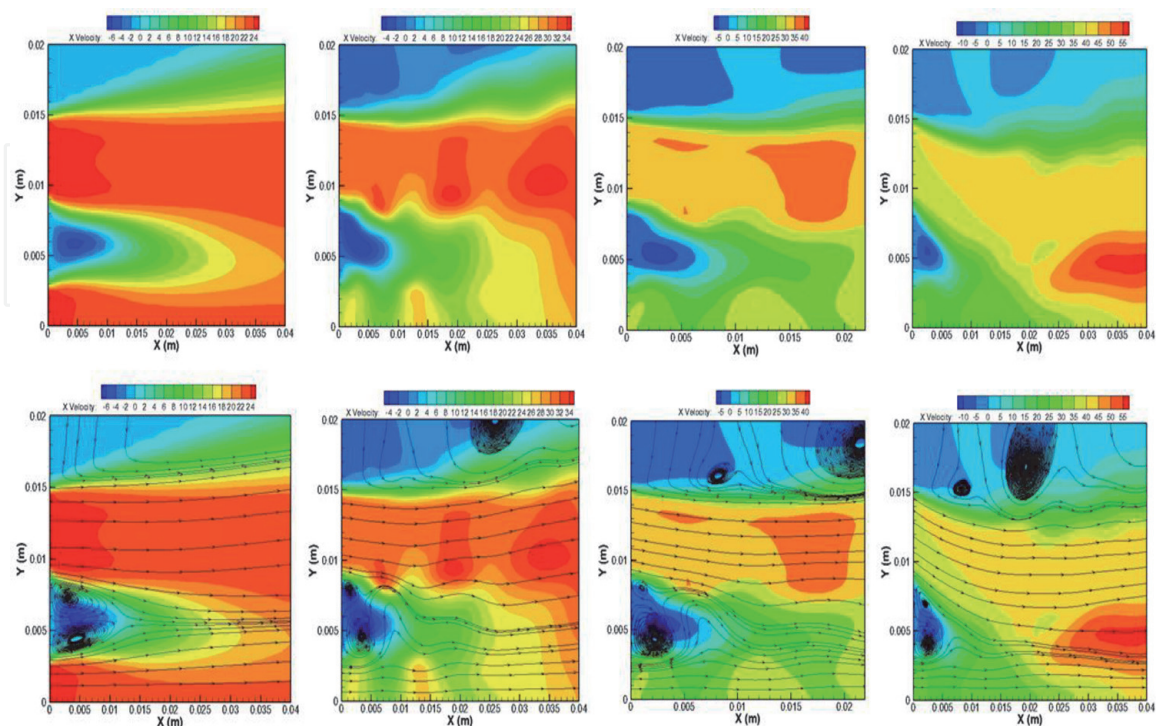


**Figure 3.**  
Velocity distribution and current lines in the combustion chamber.

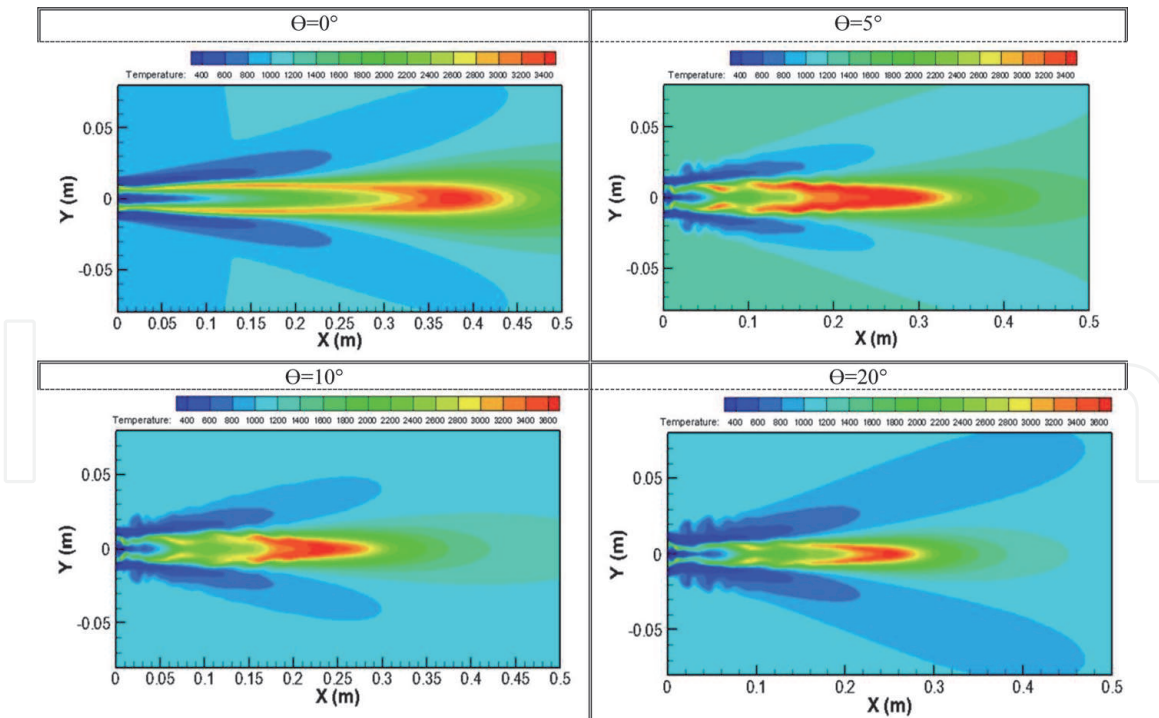


**Figure 4.**  
 Temperature distribution in the combustion chamber.

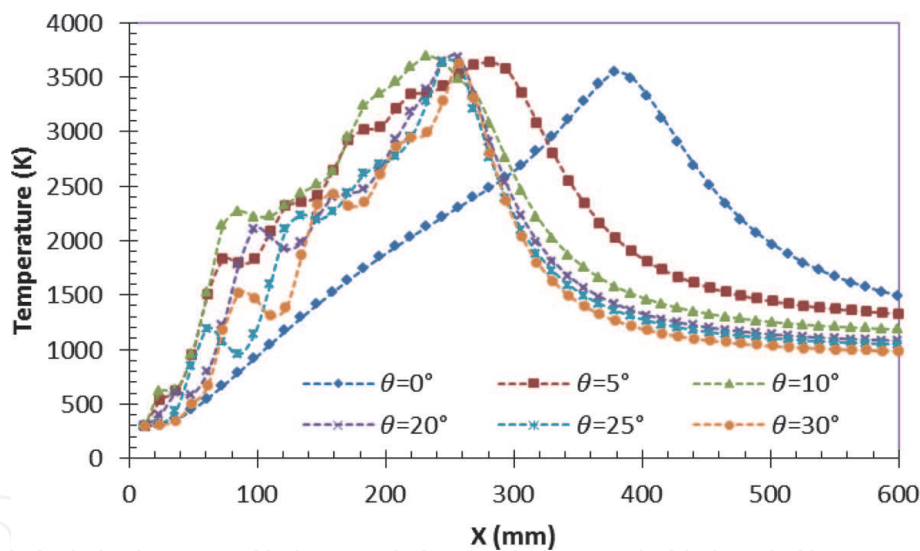


**Figure 5.**  
 Axial distribution profiles of temperature at  $y = 0$  mm with variation of the angle  $\Theta$ .

temperature increases by moving away from the burner to a maximum value and then begins to decrease. For example for  $\Theta = 0^\circ$  the temperature increases from 300 K near the burner up to 3500 K at a height of 380 mm. This zone of increase presents the mixing zone of the reactants methane/oxygen. The second zone is the reaction zone where the temperature reaches its maximum. The third zone is where the temperature gradually decreases and which presents the plume of the flame. The second interpretation is that the flame reaches its maximum faster while the angle of injection  $\Theta$  increases. Indeed, the temperature reaches its maximum at a height of 390 mm for  $\Theta = 0^\circ$  by contrast, it reaches its maximum at 260 mm for  $\Theta = 30^\circ$ . This interpretation leads to conclude that the length of the flame decreases with the increase in the angle of the oxygen jets. This result is in good agreement with the result of Boushaki [1], which showed that the average flame length



decreases when the angle of oxygen jets increases such that its value is about 500 mm for  $\Theta = 0^\circ$  and decreases until 220 mm for  $\Theta = 30^\circ$ .

## 5. Equivalence effects on dynamic

### 5.1 Radial profiles of longitudinal velocity and turbulence intensity

The radial profiles of the mean longitudinal velocity ( $U$ ) at different section ( $x/D = 1.66$ ,  $x/D = 8.33$  and  $x/D = 16.66$ ) and for three equivalence ratios are represented in **Figure 6**. A classical behavior of the multiple jets is found, one notices that the velocity profile presents maxima and minima corresponding to the three jets. In the initial zone (near the burner) each jet follows its own evolution, further downstream these velocity extremes begin to disappear to form a single maximum located in the middle of the inner mixing layer.

Near the burner ( $x/D = 1.66$ ) and for the three values of richness ( $\Phi = 1$ ,  $\Phi = 0.8$  and  $\Phi = 0.7$ ), we note that the velocity remains constant at the level of the central jet and it increases at the level of the lateral jet (jet of oxygen) with the decrease of the wealth. It should be noted that for  $\Phi = 1$  and  $\Phi = 0.7$  the mean longitudinal velocities are equal to 27 m/s and 38.57 m/s, mean velocity show an increase of 30%. In the case  $x/D = 16.66$ , the velocity profiles are slightly flattened, more open which improves the mixing of the reagents.

The influence of the equivalence ratio on the longitudinal velocity  $U$  is significant less. From an aerodynamics point of view, the decrease of equivalence ratio

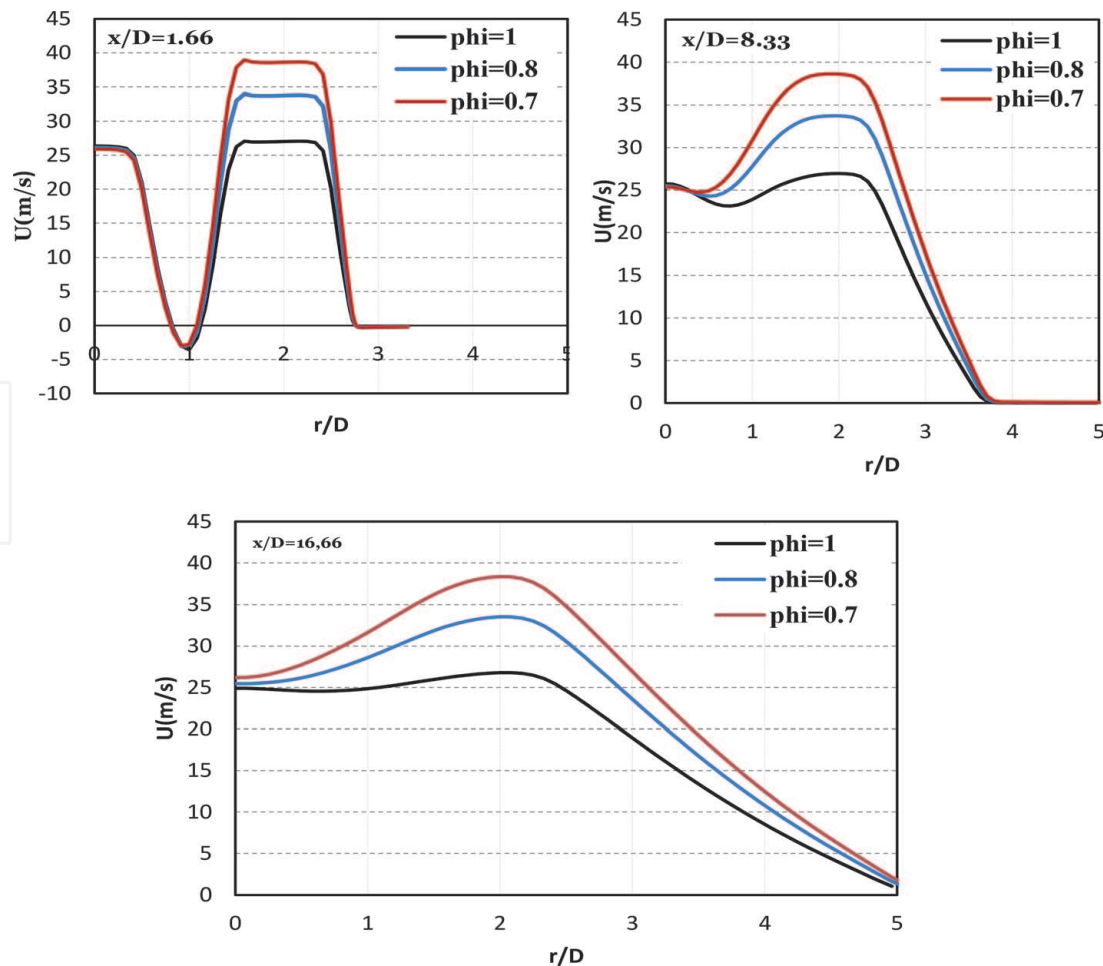


**Figure 6.** Radial profiles of longitudinal velocity at different positions from the burner.

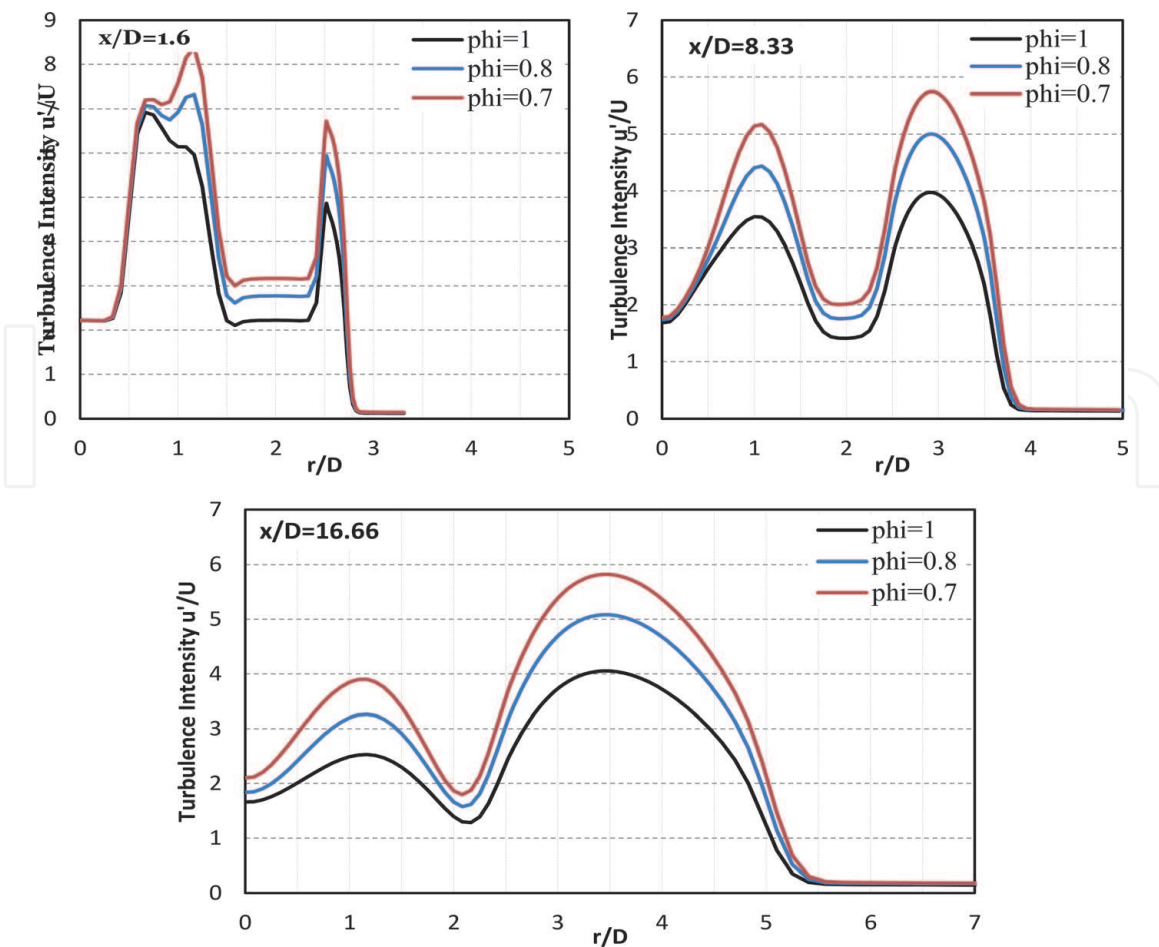


**Figure 7.**  
 Turbulence intensity at different positions from the burner.

modifies the longitudinal velocity of flow near to the burner but keep the flow velocity behavior in the combination zone.

**Figure 7** shows, the radial profiles of the turbulence intensity,  $u'/U$ , on function to the equivalence ratio and on sections different,  $x/D = 1.66, 8.33$  and  $16.66$ . In the case  $x/D = 1.66$  we see two peaks of fluctuations in  $u'$  of the order of 7 m/s, one at the center corresponding to the mixing layer of the central jet and one from the central jet corresponding to the mixture layer of side jet. These peaks of fluctuations fade along the flow with decreasing longitudinal velocity as the jets interpenetrate.

## 5.2 Radial profiles of temperature

The distribution of the temperature in sections different inside the combustion chamber, is shown in **Figure 8**. In the near of the burner, the temperature present one peak with maximum value equal to  $3000^{\circ}\text{C}$ . For a richness equal to 1 ( $\Phi = 1$ ) the maximum temperature of the adiabatic flame is  $T = 3000\text{ K}$  and for a richness 0.7 the maximum temperature equals approximately  $T = 3300\text{ K}$ . Therefore, the peaks represent the zone of the reaction between the fuel and oxidant after mixing and the region between the peaks represents the area of the fuel which is not yet burned and the reaction takes place at the interface of jets between fuel and oxidant. At  $x/D = 8.33$  and for three equivalence ratio the peak temperature is observed equal to  $3200^{\circ}\text{C}$  and the temperature profile keep constant. Far from the burner when the richness decreases, an increase in the temperature in the flame zone is observed from  $3000$  to  $3500^{\circ}\text{C}$  which makes it possible to improve the heat transfers and makes it possible to have a better thermal efficiency.

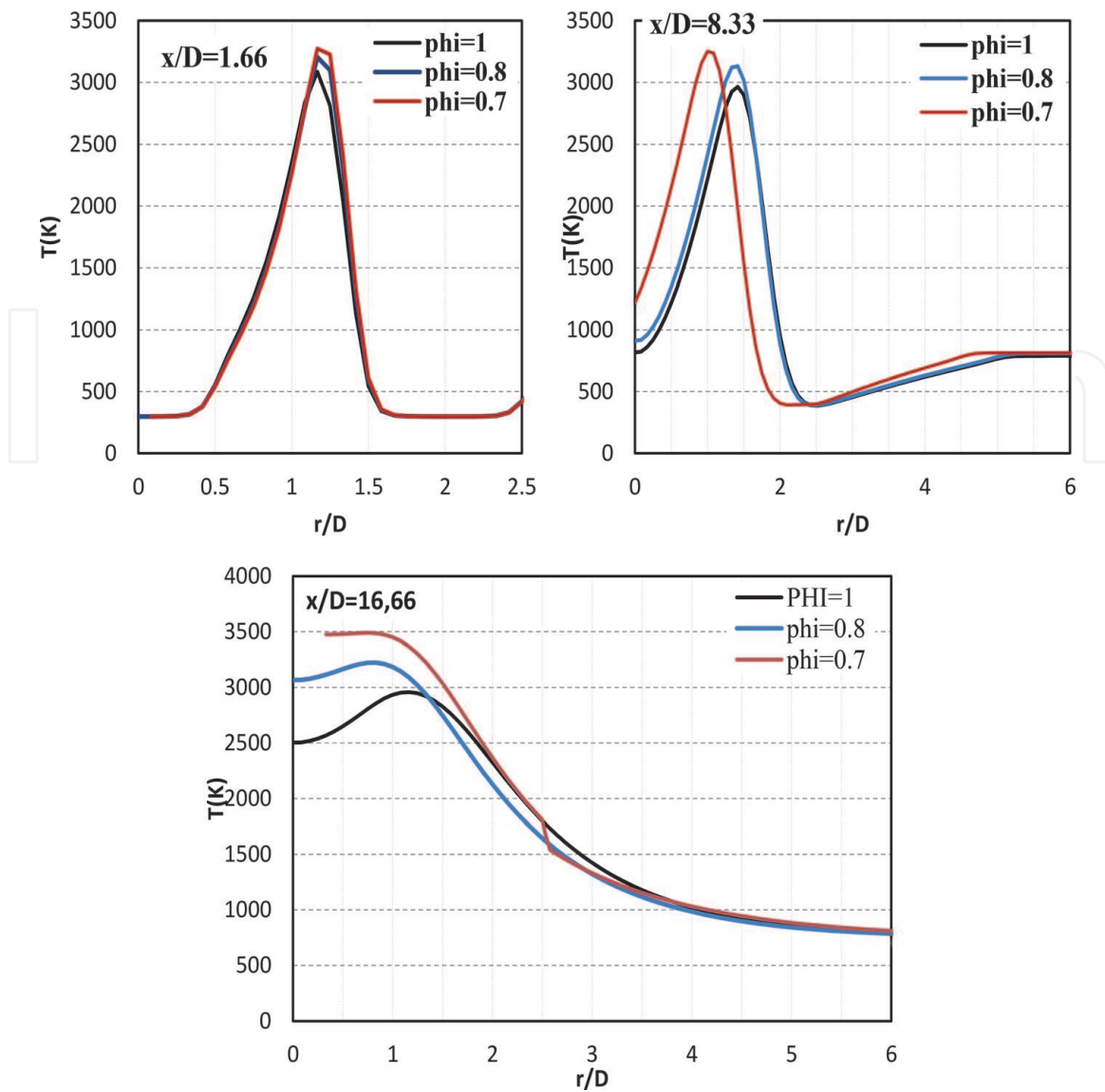


**Figure 8.**  
Radial profiles of temperature at different positions from the burner.

## 6. Effect of $H_2$ addition on the dynamic field and temperature

### 6.1 Longitudinal velocity field

**Figure 9** shows the longitudinal velocity field for different percentages of hydrogen. By comparing the four fields, the potential cone for three configurations with the addition of hydrogen percentages ( $\alpha_{H_2} = 20\%$ ,  $40\%$  and  $60\%$ ) are smaller than with pure methane. This indicates that the increase in velocity of the jet when adding hydrogen to the fuel reduces the size of the potential cone allowing the reactants to interact more effectively with oxygen and the ambient fluid. Note also that the addition of hydrogen reduces the height of the mixing area and consequently the flame height due to the high molecular diffusivity and low density of hydrogen promoting interaction between the jets more rapidly and the flow features to the behavior of a single jet.

### 6.2 Radial profiles of temperature

**Figure 10** illustrates the radial temperature profiles for multiple hydrogen percentages in the fuel mixture. This figure shows that the substitution of a fraction of

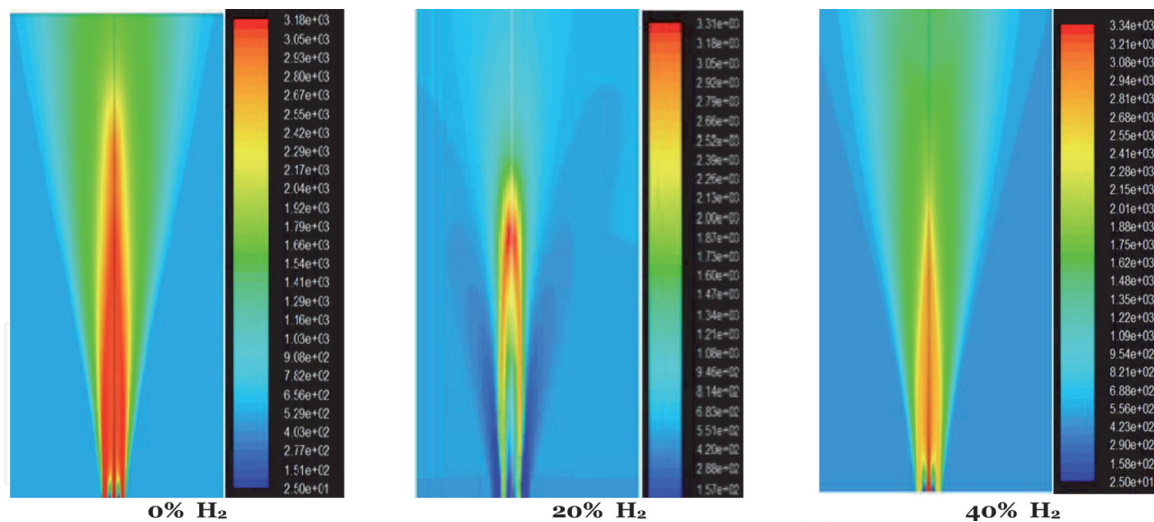


**Figure 9.**  
 Longitudinal velocity field for 0%  $H_2$ , 20%  $H_2$  and 40%  $H_2$ .

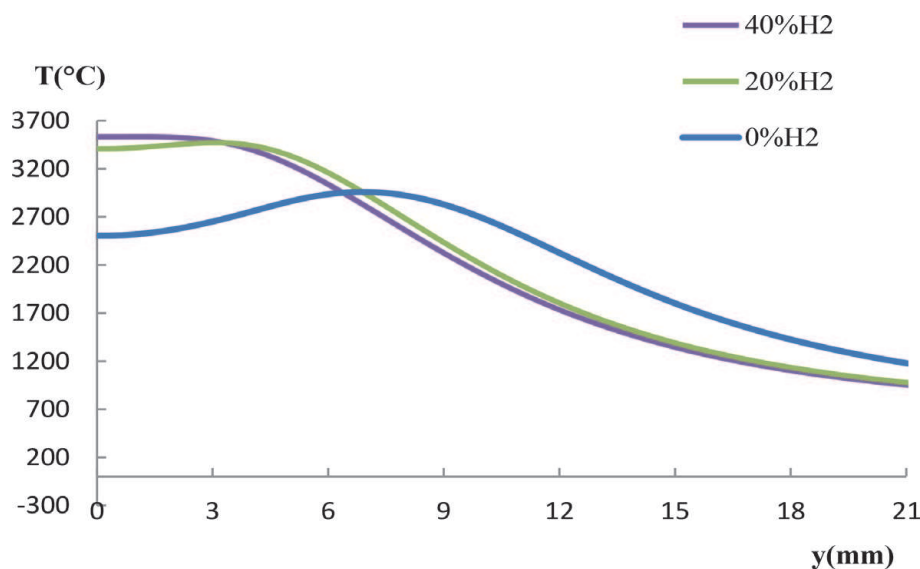


**Figure 10.**  
 Radial profiles of the temperature for 0%  $H_2$ , 20%  $H_2$ , 40%  $H_2$  and 60%  $H_2$ .

methane with hydrogen promotes the increase of the flame temperature because the calorific value of this compound is much higher than that of methane. For example, the addition of 20% hydrogen increases the temperature 2500–3400 K (up to 900 K), and the addition of 60% hydrogen increases the temperature until 3700 K (1200 K more than in pure methane combustion).

## 7. Conclusion

In this chapter, a new combustion technique in a burner with three separated jets is used. The idea of this burner consists of separating combustible and oxidant to dilute the reactants with combustion products before the mixing of the reactants. This type of burner has a great interest for the industry and the sizing of these burners requires a good understanding of the mechanisms controlling the stabilization of the flame, the release of heat and the production of pollutants.

The Particle Image Velocimetry PIV is the technique used in experimental study in non-reacting flow and reacting flow inside the combustion chamber. The Reynolds Average Navier-Stokes (RANS) method is used in this numerical simulation

with Realizable  $k-\epsilon$  as a turbulence closure model. The eddy dissipation model is applied to take into account the turbulence-reaction interactions.

The passive control added to the basic of the burner is based on the inclined of side oxygen jets towards the central natural gas jet in burner with three separated jets. From  $\Theta = 0^\circ$  to inclined state  $\Theta = 30^\circ$ , the jets fusion point becomes closer the burner as well as the dynamic field changes. The result shows that the inclination of the jets affects significantly the flow field and consequently the flame behaviour.

The effect of equivalence ratio and hydrogen on characteristics of a non-premixed oxy-methane flame from a burner with separated jets is studied in this document. The velocity fields with different equivalence ratio (0.7, 0.8 and 1) are presented. Near the burner a decrease in the equivalence ratio increases the injection velocity of the lateral jet and keeps a constant velocity in the central jet. For the turbulence intensity, near and far from the burner, an increase in the turbulence intensity is observed in the two layers of internal mixtures, this makes it possible to improve the mixing and increase the stability of the flame. Thus, there is an increase in the adiabatic temperature of the flame, which promotes heat transfer and improves thermal efficiency.

The use of hydrogen solves instability problems of the flame that are related to lean combustion, due to the high diffusivity and reactivity of hydrogen in combustion. The results showed that the addition of hydrogen increased the flame velocity and the temperature while reducing  $\text{CO}_2$  and CO emissions due to the reduction of the carbon in the fuel.

## Nomenclature

$d$	Tube internal tube, mm
$m_{ng}$	mass flow rate, $\text{kg}\cdot\text{s}^{-1}$
ng	natural gas jet
$P$	thermal power, W
Re	Reynolds number
$S$	separation distance between the jets, mm
$U_{ng}$	nozzle exit velocity of gas, $\text{m}\cdot\text{s}^{-1}$
$U_{o_2}$	nozzle exit velocity of oxygen, $\text{m}\cdot\text{s}^{-1}$
$U$	longitudinal mean velocity, $\text{m}\cdot\text{s}^{-1}$
$u'$	longitudinal velocity fluctuation, $\text{m}\cdot\text{s}^{-1}$
$V$	radial mean velocity, $\text{m}\cdot\text{s}^{-1}$
$v'$	radial velocity fluctuation, $\text{m}\cdot\text{s}^{-1}$
$r, x$	radial and longitudinal coordinate, mm

## Greek symbols

$\mu$	dynamic viscosity, $\text{kg}\cdot\text{m}\cdot\text{s}^{-1}$
$\rho$	gas density, $\text{kg}\cdot\text{m}^{-3}$
$\alpha$	percentage of hydrogen
$\Phi$	transport terms
$\Phi$	equivalence ratio
$\Gamma_\Phi$	transport coefficient

IntechOpen

## Author details

Mohamed Ali Mergheni<sup>1,2\*</sup>, Mohamed Mahdi Belhajbrahim<sup>2</sup>, Toufik Boushaki<sup>3</sup>  
and Jean-Charles Sautet<sup>4</sup>

<sup>1</sup> Department of Mechanical Engineering, College of Engineering, King Khalid University, Abha, Saudi Arabia

<sup>2</sup> College of Engineering, University of Monastir, Monastir, Tunisia

<sup>3</sup> ICARE-CNRS, Avenue de la Recherche Scientifique, University of Orléans, Orléans, France

<sup>4</sup> CORIA, CNRS-Université et INSA de Rouen, Saint Etienne du Rouvray, Rouen, France

\*Address all correspondence to: [mmerghni@kku.edu.sa](mailto:mmerghni@kku.edu.sa)

## IntechOpen

© 2020 The Author(s). Licensee IntechOpen. This chapter is distributed under the terms of the Creative Commons Attribution License (<http://creativecommons.org/licenses/by/3.0>), which permits unrestricted use, distribution, and reproduction in any medium, provided the original work is properly cited. 

## References

- [1] Boushaki T, Sautet JC, Labégorre B. Control of flames by radial jet actuators in oxy-fuel burners. *Combustion and Flame*. 2009;**156**:2043-2055
- [2] Boushaki T, Mergheni MA, Sautet JC, Labégorre B. Effects of inclined jets on turbulent oxy-flame characteristics in a triple jet burner. *Experimental Thermal and Fluid Science*. 2008;**32**:1363-1370
- [3] Das LM, Gulati R, Gupta PK. A comparative evaluation of the performance characteristics of a spark ignition engine using hydrogen and compressed natural gas as alternative fuels. *International Journal of Hydrogen Energy*. 2000;**25**:783-793
- [4] Faivre V, Poinot T. Experimental and numerical investigations of jet active control for combustion applications. *Journal of Turbulence*. 2004;**5**:5-25
- [5] Genies B. L'oxydation une solution attractive pour minimiser les émissions de NO<sub>x</sub> des procédés industriels. *Combustion et procédés industriels: Comment réduire les émissions de NO<sub>x</sub>, Rencontres et journées techniques*. A.D. E.M.E; 1996. pp. 153-196
- [6] Krothapalli A, Bagadanoff D, Karamchetti K. Development and structure of a rectangular jet in a multiple jet configuration. *AIAA Journal*. 1980;**18**(8):945-950
- [7] Lee BJ, Kim JS, Lee S. Enhancement of blow-out limit by the interaction of multiple nonpremixed jet flames. *Combustion Science and Technology*. 2004;**176**:481-497
- [8] Lenze B, Milano ME, Günther R. The mutual influence of multiple jet diffusion flames. *Combustion Science and Technology*. 1975;**11**:1-8
- [9] Lesieur C. Modélisation de la combustion turbulente non prémélangée dans un brûleur à jets séparés: Application à la stabilisation d'une oxy-flamme [PhD thesis] INSA of Rouen; 2003
- [10] BelhajBrahim MM, Mergheni MA, Ben Nasrallah S, Sautet JC. Numerical study of hydrogen enrichment effects in oxy-flame turbulent of three separated jets. *Applied Thermal Engineering*. 2017;**113**:490-498
- [11] Mergheni MA, Boushaki T, Sautet JC, Ben Nasrallah S. Numerical study of oxy-flame characteristics in a burner with three separated jets. *Applied Thermal Engineering*. 2016;**111**:49-98
- [12] Momirlan M, Veziroglu TN. The properties of hydrogen as fuel tomorrow in sustainable energy system for a cleaner planet. *International Journal of Hydrogen Energy*. 2005;**30**(7):795-802
- [13] Moawad AK, Rajaratnam N, Stanley SJ. Mixing with multiple circular turbulent jets. *Journal of Hydraulic Research*. 2001;**39**(2):163-168
- [14] Pani B, Dash R. Three dimensional single and multiple jets. *Journal of Hydraulic Engineering*. 1983;**10**:254-269
- [15] Raghunatan S, Reid IM. A study of multiple jet. *AIAA Paper*. 1981;**19**:124-127
- [16] Salentey L. Etude expérimentale du comportement de brûleur à jets séparés: application à la recherche gaz naturel-oxygène pur [PhD thesis] University of Rouen; 2002
- [17] Simonich JC. Isolated and interacting round parallel heated jets. *AIAA Paper*. 1986:86-0281
- [18] Sautet JC, Salentey L, Ditaranto M, Samaniego JM. Length of natural gas-

oxygen nonpremixed flames.  
Combustion Science and Technology.  
2001;**166**:131-150

[19] Sautet JC, Boushaki T, Salentey L,  
Labegorre B. Oxy-combustion  
properties of interacting separated jets.  
Combustion Science and Technology.  
2006;**178**:2075-2096

[20] Yimer I, Becker HA,  
Grandmaison EW. Development of flow  
from multiple jet burner. AIChE  
Journal. 1996;**74**:840-851

[21] Perthuis E. La Combustion  
Industrielle. Paris: Technip; 1983

[22] Yon S, Sautet JC. Flame lift-off  
height velocity flow and mixing of  
hythane in oxy-combustion in a burner  
with two separated jets. Applied  
Thermal Engineering. 2012;**32**:83-92

IntechOpen